

β -Catenin modulation in neurofibromatosis type 1 bone repair: therapeutic implications

Saber Ghadakzadeh,^{*,†} Peter Kannu,^{*,†,‡} Heather Whetstone,^{*} Andrew Howard,^{*,§} and Benjamin A. Alman^{*,†,¶,1}

^{*}Division of Developmental and Stem Cell Biology and [†]Institute of Medical Science, University of Toronto, Toronto Ontario, Canada; [‡]Bone Health Centre and [§]Division of Orthopaedic Surgery, Hospital for Sick Children, Toronto, Ontario, Canada; and [¶]Department of Orthopaedic Surgery, Duke University, Durham, North Carolina, USA

ABSTRACT: Tibial pseudarthrosis causes substantial morbidity in patients with neurofibromatosis type 1 (NF1). We studied tibial pseudarthrosis tissue from patients with NF1 and found elevated levels of β -catenin compared to unaffected bone. To elucidate the role of β -catenin in fracture healing, we used a surgically induced tibial fracture model in conditional knockout (KO) *Nf1* (*Nf1^{lox/lox}*) mice. When treated with a Cre-expressing adenovirus (Ad-Cre), there was a localized knockdown of *Nf1* in the healing fracture and a subsequent development of a fibrous pseudarthrosis. Consistent with human data, elevated β -catenin levels were found in the murine fracture sites. The increased fibrous tissue at the fracture site was rescued by local treatment with a Wingless-type MMTV integration site (Wnt) antagonist, Dickkopf-1 (*Dkk1*). The murine pseudarthrosis phenotype was also rescued by conditional β -catenin gene inactivation. The number of colony-forming unit osteoblasts (CFU-Os), a surrogate marker of undifferentiated mesenchymal cells able to differentiate to osteoblasts, correlated with the capacity to form bone at the fracture site. Our findings indicate that the protein level of β -catenin must be precisely regulated for normal osteoblast differentiation. An up-regulation of β -catenin in NF1 causes a shift away from osteoblastic differentiation resulting in a pseudarthrosis *in vivo*. These results support the notion that pharmacological modulation of β -catenin can be used to treat pseudarthrosis in patients with NF1.—Ghadakzadeh, S., Kannu, P., Whetstone, H., Howard A., Alman, B. A. β -catenin modulation in neurofibromatosis type 1 bone repair: therapeutic implications. *FASEB J.* 30, 3227–3237 (2016). www.fasebj.org

KEY WORDS: neurofibromin · Wnt signaling · tibial congenital pseudarthrosis · osteoblast differentiation · fracture nonunion

Neurofibromatosis type 1 (NF1) is an autosomal dominant disorder characterized by activated RAS signaling and mutations that dysregulate the NF1 protein (neurofibromin). NF1-related skeletal abnormalities are an important cause of morbidity with osteoporosis, scoliosis, and tibial dysplasia affecting more than half of affected individuals. Tibial dysplasia typically starts with anterolateral tibial bowing, characteristically progressing to a fracture that will not heal, termed a pseudarthrosis. Normal fracture healing is characterized by the deposition of

new bone from osteoblasts, followed by a period of remodeling in which osteoclasts are active. At the tibial pseudarthrosis fracture site, however, is fibrous hamartoma tissue contain cells that do not undergo osteoblastic differentiation form. There is also an increase in osteoclastogenic activity at the fracture site, when compared to the healing in a normal fractured tibia (1–4). Because tibial pseudarthrosis is refractive to medical treatment, the only management options are surgical. For those continuing to experience chronic pain and impaired mobility, an amputation may be required if other treatments are not effective.

Germline heterozygous mutations of *NF1* cause NF1. In some but not all NF1-related tibial pseudarthrosis, a second hit to the *NF1* gene resulting in biallelic inactivation of the *NF1* locus has been identified at the fracture site (5, 6). The contribution of abnormal RAS signaling in the development of NF1 tibial pseudarthrosis is well documented (7, 8). Neurofibromin (NF1 protein) is a negative regulator of the RAS-MEK signal. ERK signaling pathway and phosphorylated ERK is overactive at the pseudarthrosis site (7). NF1 mutations result in constitutive Ras activation (9) underlying the aberrant proliferation and differentiation in multiple cell types,

ABBREVIATIONS: α MEM, α -modified essential medium; μ CT, micro-computed tomography; BMD, bone mineral density; *Catnb*, β -catenin gene; CFU-F, colony-forming unit-fibroblast; CFU-OB, colony-forming unit-osteoblast; *Dkk-1*, Dickkopf-1; FBS, fetal bovine serum; GFP, green fluorescent protein; GSK3 β , glycogen synthase kinase-3- β ; KO, knockout; MOI, multiplicity of infection; MSC, mesenchymal stromal cell; NF1, neurofibromatosis type 1/neurofibromin; qRT-PCR, quantitative RT-PCR; TCP, Toronto Centre for Phenogenomics; TRAP, tartrate-resistant acid phosphatase; Wnt, wingless-type MMTV integration site

¹ Correspondence: Department of Orthopaedic Surgery, Duke University, Durham, NC 27710, USA. E-mail: ben.alman@duke.edu

doi: 10.1096/fj.201500190RR

This article includes supplemental data. Please visit <http://www.fasebj.org> to obtain this information.

including pro-osteoblasts (10) and osteoclasts (11), causing tibial pseudarthrosis.

The Wntless-type MMTV integration site (Wnt)/ β -catenin signaling pathway is critically important in skeletal development and repair. In the absence of Wnt-activating ligands, cytosolic β -catenin is targeted for ubiquitination through glycogen synthase kinase (GSK)-3 β , and the pathway is rendered inactive. β -Catenin plays a critical role in mesenchymal differentiation to osteoblasts. β -Catenin must be precisely regulated for undifferentiated mesenchymal cells to become osteochondral precursors, with elevated or decreased levels inhibiting differentiation. In contrast, β -catenin positively regulates osteoblastic differentiation in osteochondral precursor cells (12). This plays a role in fracture repair, where early on in the process, the precise regulation of β -catenin is necessary for mesenchymal cell differentiation into osteochondral progenitors (13). Later in the process, when these undifferentiated cells are committed to an osteochondral lineage, β -catenin positively regulates osteoblast differentiation. Thus, β -catenin plays a different role in the early and late stages of repair. Because β -catenin is crucial in skeletal development and repair, we hypothesized that it may also be important in NF1 pseudarthrosis. We thus investigated the role of β -catenin in NF1-associated tibial pseudarthrosis and fracture repair in mice lacking Nf1.

MATERIALS AND METHODS

Experimental animals

Mice expressing conditional *Nf1*-null alleles (*Nf1*^{fl/fl} mice) (14) were crossed with mice expressing conditional null or stabilized alleles of β -catenin. *Catnb*^{lox(ex3)} mice possess loxP sites flanking exon 3 of the β -catenin gene (*Catnb*) that result in the conditional stabilization of β -catenin in response to Cre recombination (15). The *Catnb*^{tm2Keni} mice possess loxP sequences in introns 1 and 6 of *Catnb*, which leads to a nonfunctional (null) β -catenin protein when subjected to Cre recombinase (16). All mouse strains were maintained in the C57/Bl6 background. All experiments were approved by the internal Institutional Review Board at the Toronto Centre for Phenogenomics (TCP).

Adenoviral vectors

Adenoviral vectors were purchased from Vector BioLabs (Philadelphia, PA, USA). Adenoviruses expressing GFP-tagged Cre recombinase (Ad-Cre) or a green fluorescent protein (GFP)-expressing construct (Ad-GFP) was used to induce Cre recombination, or as a control, respectively. A previously generated adenovirus containing a Dickkopf-1 (Dkk1)-expressing construct (Ad-Dkk1) was used to inhibit canonical Wnt pathway signaling locally and temporally (13, 17). The efficiency of Ad-Cre-GFP or Ad-GFP infection was measured 24 h after viral infection using a fluorescent microscope. The infection efficiency was quantified by calculating the number of GFP⁺ cells as a percentage of the number of total cells in the tissue culture well.

Detection of Cre-mediated recombination of floxed alleles

Cre-mediated recombination of the *Nf1* floxed gene was detected by using genomic PCR (14). The sequences for Nf1 PCR primers

are listed in Supplemental Table S1. Recombination efficiency was estimated with densitometry of PCR bands.

Tibial fracture model

A unilateral (right side) open transverse tibial fracture with intramedullary needle fixation was used as the bone fracture model, similar to that described elsewhere (13). Twelve-week-old male mice were used for these experiments. The fractures were stabilized with a 0.3 mm insect pin (Austerlitz insect pin, size 00; Entomoravia, Slavkov u Brna, Czech Republic). A preparation of either Ad-Cre-GFP or Ad-GFP (2×10^8 pfu) mixed with 10 μ l of Matrigel (BD Biosciences, Franklin Lakes, NJ, USA) was injected into the induced fracture gap. For mice treated with Ad-Dkk1, 2×10^7 pfu of Ad-Dkk1 was added to the Ad-Cre-GFP and Matrigel mixture. Ad-GFP was used as the control. The mice were euthanized and fractures harvested for analysis at various time points after injury.

Radiographic and micro-computed tomography analysis

Radiographs were obtained with a Faxitron X-ray machine (model MX20; Faxitron X-ray Corp., Tucson, AZ, USA). Micro-computed tomography (μ CT) analyses were performed using a SkyScan 1174 compact μ CT scanner (SkyScan, Kontich, Belgium). Images were reconstructed with the NRecon software (SkyScan) and analyzed using CTAn software version 1.13.2.1 (SkyScan). The reconstructed images were then color coded according to the bone mineral density (BMD) values measured by BMD phantom-calibrated μ CT. The volume of interest for quantitative analysis was defined as extending 1 mm proximally and distally from the line of fracture within the callus region along the periosteum. At least 7 samples were used in each group for the analysis.

Histology and histomorphometry

Bone samples were harvested for histologic analysis. Tissues were fixed in 4% normal-buffered formaldehyde decalcified in 20% EDTA (pH 8.0) and then embedded in paraffin. Serial sections of 5 μ m were deparaffinized, rehydrated to water, and stained with toluidine blue, safranin O, or tartrate-resistant acid phosphatase (TRAP). An average of 10 tissue sections were used to measure histomorphometric parameters of callus. The number of osteoblasts per bone surface area and the number of osteoclasts per bone surface area were counted at 2 locations per section in 6 animals in each experimental group; quantification of the cells was performed as has been described (13) and according to the standard protocols recommended by the American Society for Bone and Mineral Research (18). The region of interest was selected as containing 6 microscope fields at $\times 20$ magnification, measuring ~ 1.6 mm², established at the site of fracture. Histomorphometry was undertaken as previously reported (19). Osteoblasts and osteoclasts were quantified in each sample, and the results were normalized against corresponding bone area (mm²) in the same sample.

Biomechanical torsion testing

Biomechanical torsion testing was performed on an MTS Bionix 858 materials-testing system (MTS Systems, Eden Prairie, MN, USA). The tibiae were potted proximally and distally, keeping a consistent gauge length of 7 mm with the fracture line in the

middle. Torque was measured using a 1.4 N·m reaction torque transducer (Futek, Irvine, CA, USA) during the application of angular displacement ($1^\circ/\text{s}$) until failure.

Cell culture

Bone marrow cells were extracted from mouse long bones (femora and tibiae) by flushing the long bones with α -modified essential medium (α MEM) with 1% antibiotics and antimycotics and 10% fetal bovine serum (FBS; Thermo Fisher Scientific Life Sciences, Mississauga, ON, Canada). The cells were then counted and plated in 6-well plates at a density of $1 \times 10^6/\text{well}$ and grown for 5 d in α MEM supplemented with 10% FBS. The cells were transfected with 250 multiplicity of infection (MOI) of Ad-Cre or Ad-GFP at d 5 of the culture. One week after adenoviral infection experiment, cell viability was determined by trypan blue exclusion assay (Sigma-Aldrich Canada, Oakville, ON, Canada) (20). In brief, the medium was removed from each well, and the cells were rinsed with PBS, after enzymatic release of the adherent cells by trypsin/EDTA solution [0.025% trypsin and 0.01% EDTA (Thermo Fisher Scientific Life Sciences)] 50 μl aliquots of cell suspension from each well was incubated with 50 μl 1% trypan blue (Sigma-Aldrich Canada) for 5 min at room temperature. Dead cells, with blue staining were counted on a hemocytometer and the percentage of viable cells was calculated *vs.* the total number of cells counted. After verifying adenoviral infection, osteogenic medium containing 50 $\mu\text{g}/\text{ml}$ of ascorbic acid, 10 mM β -glycerophosphate, and 1×10^{-8} M dexamethasone was started at d 7 and continued for 14 d to induce osteogenesis. The medium was refreshed every 48 h. For colony-forming unit (CFU) analysis, the medium was removed, the plates were rinsed with $1 \times$ PBS, and the cells were fixed with 10% formalin for 30 min and then rinsed with distilled water 3 times. For colony-forming unit fibroblast (CFU-F) analysis, the cells were stained with crystal violet (Sigma-Aldrich) solution (0.5 g/100 ml methanol) for 30 min, washed with distilled water 3 times and air dried in a fume hood overnight. To determine osteogenic differentiation and matrix mineralization by colony-forming unit osteoblasts (CFU-OBs), cells were stained with Alizarin Red stain. Fixed cells were stained with a 1 g/100 ml water solution of Alizarin Red S (Sigma-Aldrich; pH 4.1–4.3) for 30 min at room temperature. The cells were then rinsed with distilled water until all the excess unattached stain was removed and the rinsed water was clear. CFU analyses were performed by counting the number of stain-positive colonies with more than 50 cells under a light microscope.

Human samples

Primary human bone marrow cells, bone samples, or tibial pseudarthrosis tissue samples were obtained from patients with NF1 undergoing surgery for the pseudarthrosis. Bone marrow cells were also obtained from age-matched patients who did not have any known genetic disorder and were undergoing orthopedic surgery for other reasons. Human ethics approval was obtained from the Hospital for Sick Children (Toronto, ON, Canada). Cells were isolated with Ficoll Paque (GE Healthcare, Pittsburgh, PA, USA) density gradient centrifugation, according to the manufacturer's protocol, and cultured in 6-well plates at a density of 5000 cells/well in α -MEM, GlutaMax (Thermo Fisher Scientific Life Sciences) with antibiotics-antimycotics and 10% FBS (Thermo Fisher Scientific Life Sciences). Osteogenic medium consisting of α MEM (high glucose, glutamine), 1% antibiotics-antimycotics, 10% heat-inactivated FBS, dexamethasone (1×10^{-7} M), β -glycerophosphate (10 mM), and ascorbic acid (50 $\mu\text{g}/\text{ml}$) was used

from d 7 to 24 of the culture. To modulate Wnt signaling, cells either received a single dose of 50 ng/ml of the recombinant Wnt-3a (R&D Systems, Minneapolis, MN, USA) or were treated with 250 MOI of either Ad-Dkk1 or Ad-GFP.

Protein analysis

Western blot analysis was performed in triplicate on human and mouse tissues to assess intracellular levels of β -catenin. Protein was obtained using the Reporter Gene Assay Lysis Buffer (Roche Applied Science, Indianapolis, IN, USA) and quantified by the bicinchoninic acid protein assay (Thermo Fisher Scientific Life Sciences). Primary antibodies against total β -catenin (Upstate Biotechnology, Lake Placid, NY, USA) and Actin (Calbiochem, San Diego, CA, USA) were used. Horseradish peroxidase-tagged secondary antibodies and ECL (GE Healthcare) were used to detect hybridization. Densitometry was performed with AlphaEaseFC software (Alpha Innotech Corp., San Leandro, CA, USA).

Quantitative gene expression analysis

Tissues were snap frozen in liquid nitrogen and processed with the BioPulverizer (Thomas Scientific, Swedesboro, NJ, USA). Total RNA was isolated with TRIzol Reagent (Thermo Fisher Scientific Life Sciences), according to the manufacturer's protocol. Total RNA was reverse transcribed into cDNA with the Superscript II kit (Thermo Fisher Scientific Life Sciences) as per the manufacturer's protocol. Target and endogenous control genes were amplified by using TaqMan primers (Thermo Fisher Scientific Life Sciences). All reactions were run in duplicate with a 7900HT Fast Real-Time PCR System (Thermo Fisher Scientific Life Sciences). Differential expression was determined using the comparative C_t method. TaqMan primers used for quantitative (q)RT-PCR are listed in Supplemental Table 2.

Statistical analysis

Results are presented as means \pm SD. Statistical analyses included unpaired Student's *t* tests and 1-way ANOVA followed by Tukey's *post hoc* test. Results reaching $P < 0.05$ were significant.

RESULTS

β -Catenin protein level is elevated in tibial pseudarthrosis tissue

Four children with NF1, diagnosed by standard criteria, and affected by tibial pseudarthrosis, were studied. Genotyping studies by Sanger sequencing, confirming an NF1 mutation, did not reveal NF1 loss of heterozygosity. β -Catenin levels in pseudarthrosis tissue were compared by Western blot analysis to adjacent unaffected bone from the same patient. Total β -catenin protein levels were 4 times higher in pseudarthrosis tissue when compared with adjacent unaffected bone tissue (Fig. 1A). Increased β -catenin protein levels were associated with an increased expression of the Wnt target gene *AXIN2*, indicating up-regulation of the β -catenin transcriptional activation (Fig. 1B). Tibial pseudarthrosis in a mouse was analyzed in a similar manner. The tibial diaphysis of *Nf1^{fllox/fllox}* mice was fractured by using a reported technique (13). Ad-Cre viral infection was used to induce

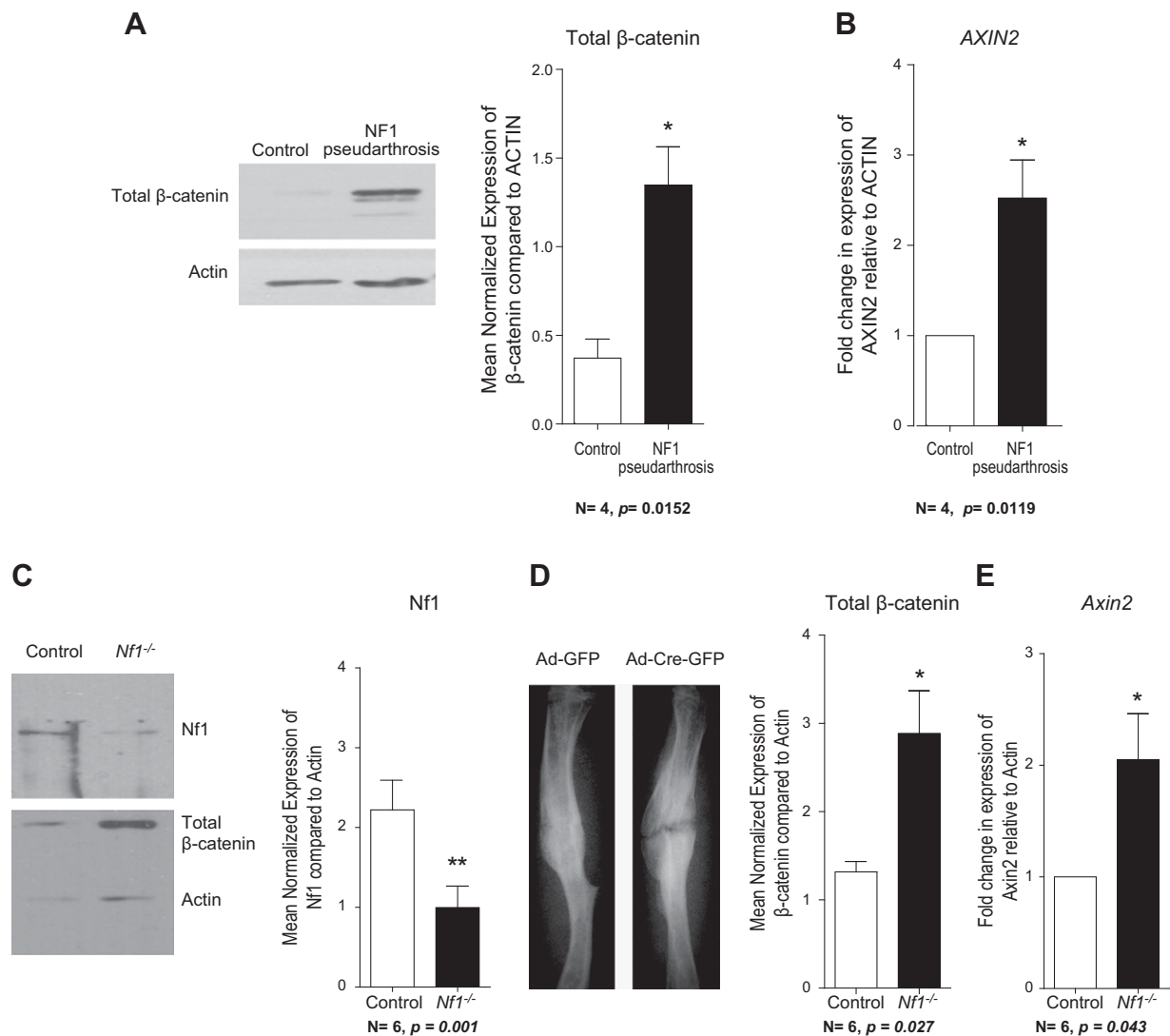


Figure 1. The β-catenin protein level is increased in tibial pseudarthrosis tissue. *A*) Representative image of Western blot analysis showing total β-catenin protein levels in NF1 patient tibial pseudarthrosis tissue, with unaffected bone tissue as the control. The graph shows the results from 4 independent NF1 pseudarthrosis samples and 4 unaffected bone samples as controls. *B*) qPCR results from human NF1 tibial pseudarthrosis tissue ($n = 4$) and unaffected bone samples as controls ($n = 4$). The experiment was undertaken with 3 technical replicates. There was a significant increase in *AXIN2*, a downstream target of the canonical Wnt signaling pathway in NF1 pseudarthrosis tissue. *C*) Representative image of Western blot analysis shows an increase in cellular β-catenin levels at the *Nf1*^{-/-} fracture site compared to wild-type fractures. *D*) *Nf1*^{flox/flox} mice were used to determine the effects of Nf1 on β-catenin changes. Either Ad-GFP or Ad-Cre-GFP was used locally on the fracture site. Representative X-ray images of fractured tibiae in *Nf1*^{flox/flox} mice, treated with Ad-GFP or Ad-Cre-GFP. Unlike *Nf1*^{flox/flox} (left radiograph), *Nf1*^{-/-} (right radiograph) tibial fractures did not heal after 21 d and developed a nonunion phenotype similar to human pseudarthrosis (right radiograph). *E*) qPCR results showing a significant increase in the gene expression of *Axin2* at the *Nf1*^{-/-} fracture site. Data are expressed as means ± 95% CI of 4 human or 6 mouse samples per experimental condition. * $P < 0.05$; ** $P < 0.01$.

recombination in fractures from *Nf1*^{flox/flox} mice and verified by PCR (Supplemental Fig. 1). Western blot analysis demonstrated a loss of neurofibromin at the fracture site (Fig. 1C). Mice with deficient Nf1 at the site of the tibial fracture exhibited decreased ossification 21 d after fracture when compared with *Nf1*^{flox/flox} controls infected with Ad-GFP, as shown by radiographs (Fig. 1D), fracture site histology showing increased fibrocartilage (see Fig. 3B) and a μ CT scan analysis revealed a less-mineralized callus (see Fig. 3C). Western blot and qPCR analyses showed that β-catenin protein and *Axin2* levels were higher in the *Nf1*-null murine fracture site tissue, respectively (Fig. 1E).

β-Catenin is elevated during osteoblastic differentiation in neurofibromatosis

We next studied the differentiation of progenitor cells to osteoblasts using bone marrow aspirates from the iliac crest site in 4 patients with NF1. Control bone marrow samples were obtained from 4 healthy age- and sex-matched children. Equal numbers of CFU-F suggested an equal number of MSCs in the bone marrow aspirates from healthy patients and those with NF1. β-Catenin levels were at least twice as high during differentiation into osteoblasts in cell cultures from patients with NF1 compared

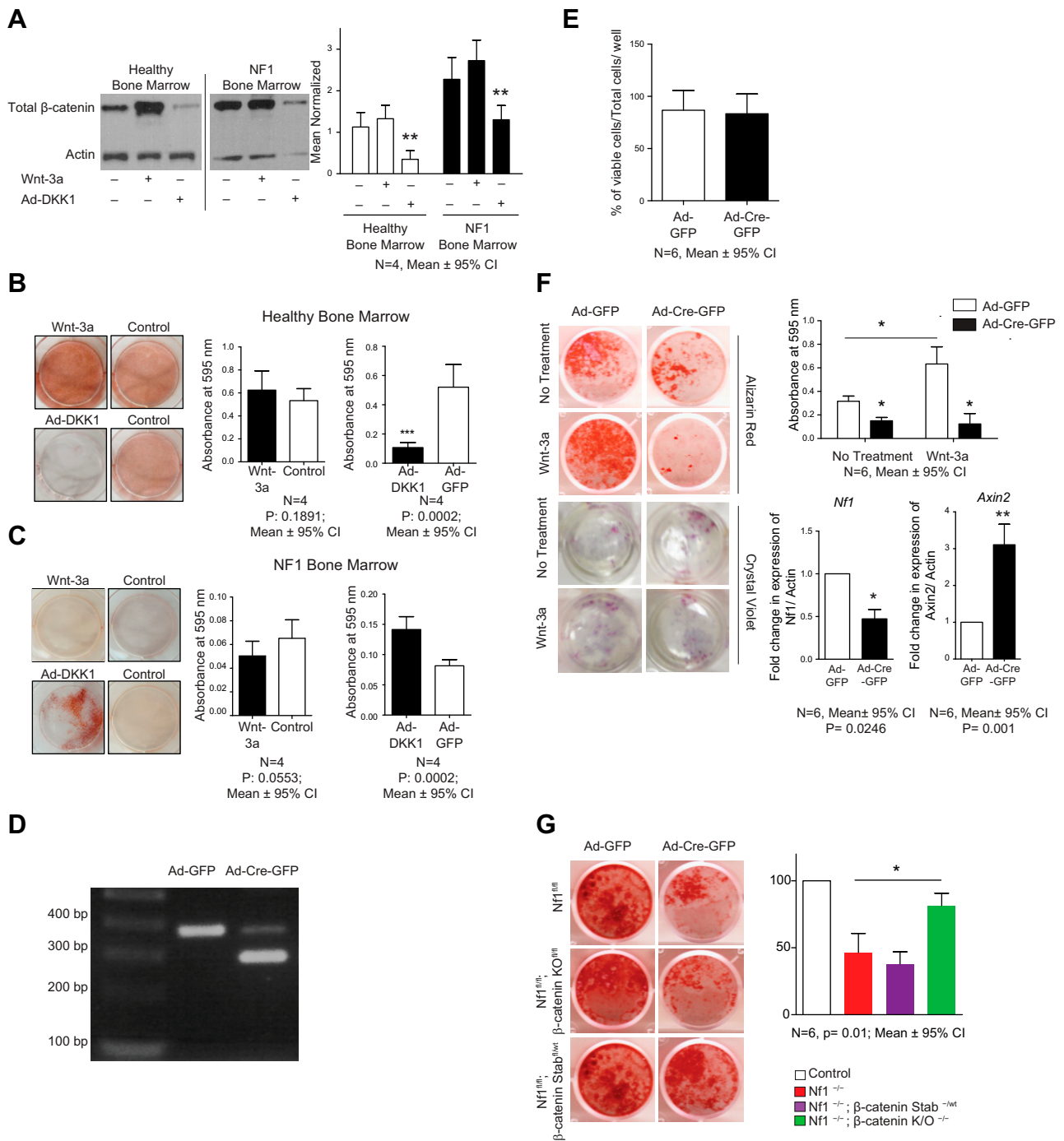


Figure 2. β -Catenin levels regulate osteoblastic differentiation in NF1. **A**) Western blot analysis (left) and densitometry (right) showing total β -catenin protein levels in cultured bone marrow–derived cells from healthy and NF1-affected individuals, treated with Wnt-3a or Ad-Dkk-1. **B**) Alizarin Red staining showed that Dkk-1, but not rWnt-3a, rescued matrix mineralization of cultured NF1 bone marrow MSCs. Graphs show colorimetric measurement of eluted mineral extracts stained with Alizarin Red, quantification of absorbance at 595 nm using a spectrophotometer. **C**) Alizarin Red staining shows that Dkk-1 suppressed mineralized matrix production of cultured bone marrow MSCs from healthy individuals. Graphs show quantification of spectrophotometer colorimetry. **D**) Ad-Cre-mediated recombination of the conditional *Nf1* flox allele detected using genomic PCR. Recombination efficiency estimated by calculating the density of the 280 bp deletion band as a percentage of the total density of both recombined and nonrecombined (350 bp) bands. Mean recombination efficiency was 85% in Ad-Cre-GFP group (95% CI = 74–96). **E**) Cell viability after adenoviral infection. Data from the trypan blue assay showed no significant difference in the percentage of viable cells in the Ad-GFP- and Ad-Cre-GFP-treated groups, 1 wk after adenoviral infection. **F**) Alizarin Red staining and release assay of *Nf1*^{+/+} bone marrow MSCs differentiated in OB medium and treated with either Ad-Cre-GFP or Ad-GFP. Wnt/ β -catenin was up-regulated by a single pulse of rWnt-3a treatment. *Nf1*^{-/-} MSCs failed to differentiate into osteoblasts, and less mineralization was observed compared with the control. rWnt-3a treatment further inhibited mineralization in the *Nf1*^{-/-} group. **G**) Alizarin Red staining of mouse bone marrow MSCs, differentiated into osteoblasts. The graph shows the percentage of CFU-Os in different groups compared with their controls. *Nf1*^{-/-} MSCs failed to differentiate into osteoblasts as efficiently as wild-type (continued on next page)

to controls (Fig. 2A). Similar to previous reports (1, 21, 22), osteoblastic mineralization was diminished in patients with NF1 cultures compared to controls (Fig. 2B, C). To evaluate the role of Nf1 in murine osteoblast differentiation, we harvested primary MSCs from *Nf1^{fllox/fllox}* mice and transduced these cells with a Cre-expressing adenovirus, Ad-Cre. More than 90% of cells were infected, as quantified with fluorescence microscopy (Supplemental Fig. S3). Cre-mediated recombination of the conditional *Nf1* floxed alleles occurred in 85% of the cells, as determined by PCR (95% CI, 74–96%; Fig. 2D). Data from the trypan blue assay showed no significant difference in the percentage of viable cells in Ad-GFP- and Ad-Cre-GFP-treated groups, 1 wk after adenovirus infection (Fig. 2E). We found a 50% decrease in the mineralized matrix when Nf1 was knocked down, confirmed by an Alizarin Red release assay (Fig. 2F). During differentiation, β -catenin and *Axin2* levels were elevated 3-fold in samples in which Nf1 was knocked down compared to control samples (Fig. 2F). Taken together, the data show that β -catenin levels are elevated during *in vitro* osteoblastic differentiation in neurofibromatosis.

β -Catenin down-regulation enhances osteogenic differentiation

To investigate the functional implications of β -catenin on osteogenic differentiation in NF1, human cells were either treated with rWnt3A or infected with Ad-Dkk1. rWnt3A will increase β -catenin protein level, whereas Dkk1 will inhibit β -catenin protein levels, through modulation of the canonical Wnt pathway. Dkk-1 inhibited β -catenin, resulting in a 50% decrease in β -catenin levels, whereas treatment with rWnt3A caused a 20% increase in β -catenin (Fig. 2A). In bone marrow samples from controls, infection with Ad-Dkk-1 suppressed matrix mineralization, whereas treatment with rWnt3A increased matrix mineralization (Fig. 2B). However, the results were opposite when the identical treatments were undertaken with NF1 bone marrow cells. Ad-Dkk1 infection of osteoblasts from patients with NF1 resulted in a mineralized matrix, but Wnt3A had no effect on mineralization (Fig. 2C).

Next, we studied differentiation into osteoblasts in *Nf1^{fllox/fllox}* mice with β -catenin levels altered by rWnt-3a. Calcified matrix production was determined by Alizarin Red staining and release assay. We found that rWnt-3a did not increase matrix mineralization in *Nf1^{-/-}* osteoblasts the way it did in the control cells (Fig. 2F).

We then generated conditional mice in which we could regulate both β -catenin and *Nf1*. *Catnb^{tm2Kem}* mice, which express a null β -catenin protein after Cre recombination (23). As a control, we also analyzed *Catnb^{lox(ex3)}* mice, which express a stabilized β -catenin protein levels after Cre recombination (15). These mice were crossed with *Nf1* conditional knockout (KO) mice. Bone marrow cells isolated from *Nf1^{fl/fl}*, *Nf1^{fl/fl};Catnb^{lox(ex3)}*, and *Nf1^{fl/fl};Catnb^{tm2Kem}*

mice were cultured and transfected *ex vivo* with either Ad-Cre or Ad-GFP. Bone marrow cells were plated at the same density for differentiation into osteoblasts. CFU-O numbers were quantified by counting the Alizarin Red-positive colonies (Fig. 2G). *Nf1*-null cultures expressing no β -catenin showed an increased number of CFU-Os *vs.* control cultures, whereas there was not a statistically significant difference in cultures expressing the stabilized allele. Thus, inhibition of β -catenin stimulates differentiation into osteoblasts in Nf1-deficient cells.

Reduced β -catenin levels enhance fracture healing in an Nf1 murine model

To determine the role of β -catenin in fracture repair in Nf1 *in vivo*, we examined tibial fracture healing in the compound mutant mice. As reported (4), inactivation of Nf1 in *Nf1^{fl/fl}* mice with Ad-Cre was associated with nonunion of the fracture (Fig. 3A). Safranin O staining of the fracture site histology showed increased fibrocartilage at a time point when most of the cartilage callus was replaced by newly formed woven bone in control samples (Fig. 3B). μ CT scan analysis revealed a less mineralized callus, consistent with the histologic findings of less ossification at the fracture site (Fig. 3C).

To study the effects of β -catenin protein levels on fracture healing in NF1, we induced tibial fractures in *Nf1^{fl/fl};Catnb^{lox(ex3)}* and *Nf1^{fl/fl};Catnb^{tm2Kem}* mice and infected the fracture sites with Ad-Cre. Tibial fractures in mice with inactivation of Nf1 and inactivation of β -catenin (*Nf1^{fl/fl};Catnb^{tm2Kem}*) showed improved healing 21 d after the fracture, compared to *Nf1^{fl/fl}* mice expressing wild-type β -catenin alleles (Fig. 3A). The amount of fracture site callus fibrocartilage was significantly reduced in these mice, confirming improved fracture healing in mice expressing low levels of fracture site β -catenin (Fig. 3B). In contrast, tibial fractures in mice with inactivation of Nf1 and stabilized β -catenin (*Nf1^{fl/fl};Catnb^{lox(ex3)}*) did not heal after 21 d (Fig. 3A). We next explored the effects of an adenovirus that expressed Dkk-1, a negative regulator of the canonical Wnt pathway, on fracture repair in *Nf1^{fl/fl}* mice. Mice infected with Ad-GFP were used as controls *vs.* this group. Radiology and histologic findings revealed that bone repair was improved with the local application of an adenovirus expressing Dkk-1 (Fig. 3A, B). The amount of fracture site fibrocartilage was reduced to levels similar to the control. μ CT scan analysis of the fracture site confirmed an increase in mineralized tissue at the fracture site (Fig. 3C).

β -Catenin levels affect osteoclasts and their number in Nf1-null fracture sites

Fracture healing is dependent on the activity of several cell types, including osteoblasts that produce new bone and those that are responsible for resorbing bone. We quantified

osteoblasts. A further decrease in CFU-O number occurred with β -catenin up-regulation. β -catenin down-regulation rescued osteoblast differentiation of *Nf1^{-/-}* MSCs, but a significant difference between the number of CFU-Os was not observed. Stab, stabilized. Data are expressed as means \pm 95% CI of 4 human samples or 6 mice per experimental condition; *in vitro* experiments were performed in triplicate for each biologic human or mouse sample. * $P < 0.05$; ** $P < 0.01$; *** $P < 0.0001$.

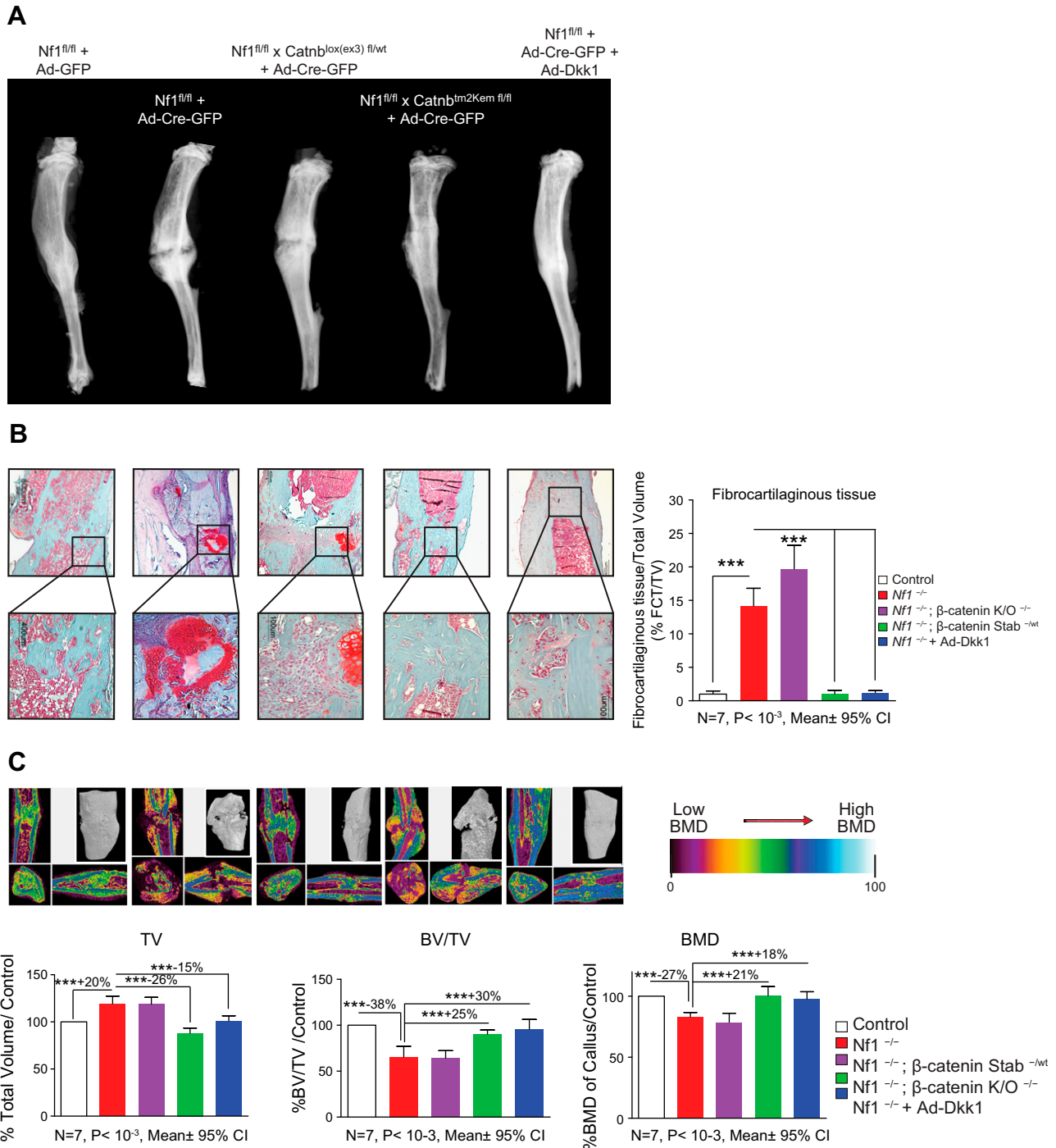


Figure 3. Reduced β -catenin levels enhance fracture healing in an *Nf1* murine model. **A)** Representative X-ray, histology, and μ CT scan of tibiae 21 d after fracture show decreased ossification in the bony callus formation in the *Nf1*^{-/-} and *Nf1*^{-/-} tibiae. β -Catenin stabilized fractures, with a gap and a significant amount of fibrocartilaginous tissue remaining at the fracture site. **B)** Histomorphometry analysis shows a significant amount of fibrocartilaginous tissue formation at the site of fracture in *Nf1*^{-/-} mice, which was eliminated by β -catenin down-regulation in transgenic *Nf1*^{-/-} and β -catenin-KO mice, and also those with Dkk-1 applied at the site of *Nf1*^{-/-} fractures. **C)** μ CT scan analysis revealed that *Nf1*^{-/-} and *Nf1*^{-/-} β -catenin-stabilized (β -catenin Stab) fractures produce significantly larger, less mineralized calluses than do their controls. This phenotype was rescued by β -catenin down-regulation in both β -catenin-KO and Ad-Dkk-1-treated *Nf1*^{-/-} groups, evidenced by higher bone volume/total volume (BV/TV) and higher BMD of the calluses. Data are expressed as means \pm 95% CI of 7 mice per experimental condition. ****P* < 0.0001.

the respective number of osteoblasts and osteoclasts from histology sections of the healing fractures at 21 d after fracture. Osteoblasts and TRAP⁺ active osteoclasts were quantified in a region containing 6 microscope fields at $\times 20$ magnification, measuring ~ 1.6 mm² in 6 different animals.

Fractures in *Nf1*-KO mice with different levels of β -catenin were compared. The number of osteoblasts was reduced in the *Nf1*-KO fracture sites. The number of osteoblasts was significantly increased in *Nf1*-KO fractures when β -catenin levels were knocked down, but they were decreased when

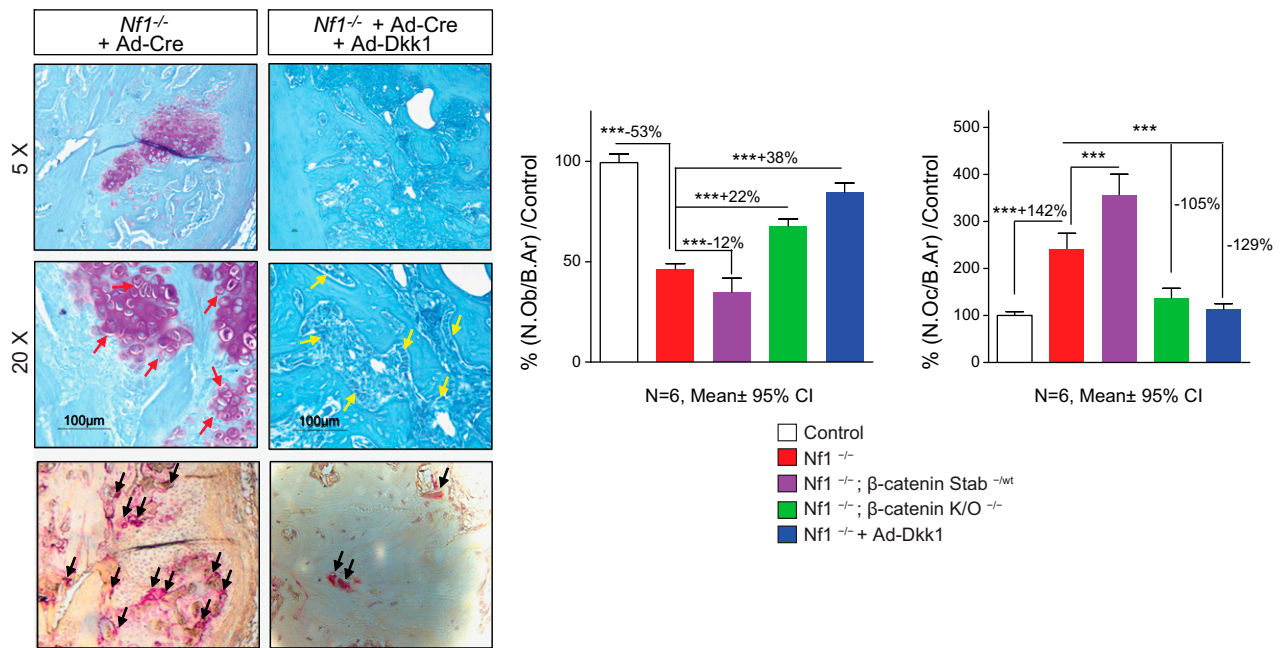


Figure 4. β -Catenin levels affect the number of osteoblasts and osteoclasts in *Nf1*-KO fracture sites. Representative histology slides showing the bone sections stained with toluidine blue (top 4 panels) or TRAP (bottom) staining 21 d after fracture. Osteoblasts (yellow arrows) and TRAP⁺ active osteoclasts (black arrows) were quantified on a region of interest containing 6 microscope fields at $\times 20$ magnification, measuring $\sim 1.6 \text{ mm}^2$ established at the site of fracture, with the line of fracture in the middle. The number of osteoblasts per bone surface area (N.Ob/B.Ar) was significantly decreased in the *Nf1*^{-/-} fractures and further decreased by stabilizing β -catenin (β -catenin Stab) at the fracture site. The number of osteoblasts was improved significantly by down-regulation of β -catenin in the β -catenin-KO mice and was further rescued by the transient down-regulation of β -catenin using Ad-Dkk1 at the fracture site. Active osteoclasts are abundant in *Nf1*^{-/-} fractures, but the number of osteoclasts per bone surface area (N.Oc/B.Ar) decreased significantly with Ad-Dkk1 treatment. Data are expressed as means \pm 95% CI of 6 mice per experimental condition. *Nf1*^{-/-} fractures also exhibit hypertrophic chondrocytes (red arrows). *** $P < 0.0001$.

β -catenin was elevated (Fig. 4). The number was significantly increased in *Nf1*-null fracture sites, but decreased when β -catenin levels were reduced.

β -Catenin inhibition improved torque and stiffness of *Nf1*-deficient fractured tibia

Biomechanical testing of fractured tibiae was undertaken to determine differences in torsional strength.

We compared *Nf1*-deficient fractures with those also treated with Dkk-1 or those that expressed conditional null alleles of β -catenin. There was a significant increase in both ultimate torque and stiffness in *Nf1*-deficient fractured tibiae with low levels of β -catenin (Fig. 5). Thus, in addition to altering histologic characteristics, inhibition of β -catenin improves in the mechanical characteristics of bone healing in NF1.

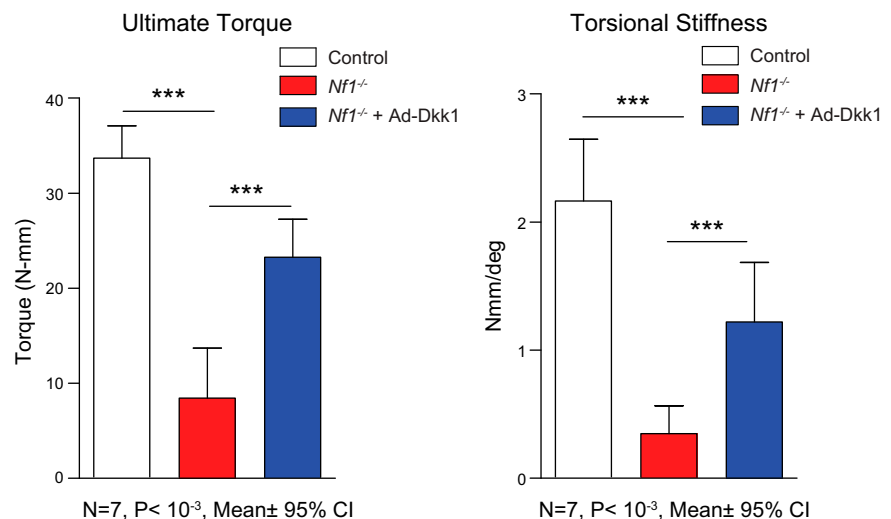


Figure 5. β -Catenin down-regulation improves torque and stiffness of *Nf1*-deficient fractured tibia. Biomechanical testing of fractured *Nf1*^{-/-} mouse tibiae revealed a significant increase in torsional stiffness after β -catenin down-regulation at the site of fracture ($n = 7$, means \pm 95% CI). *** $P < 10^{-3}$.

DISCUSSION

In this study, the β -catenin protein level was elevated in NF1-related pseudarthrosis. In mice lacking Nf1, fracture repair was associated with poor osteogenesis and low mineralized matrix production. There was substantially more hypertrophic cartilage at the murine fracture site 21 d after fracture in cases lacking *Nf1* than in the controls. This observation is consistent with a change in the fate of mesenchymal precursor cells, inhibiting osteoblastic differentiation. Reducing β -catenin levels at the murine *Nf1*-KO fracture site enhanced fracture healing *in vivo*. Thus, the fracture repair phenotype is partially mediated by dysregulated β -catenin.

One possibility is that Nf1 directly regulates β -catenin, causing the observed phenotype. For example, a downstream component of RAS, the serine/threonine kinase AKT, can regulate β -catenin-dependent transcription by inhibiting GSK-3 β , by directly activating β -catenin, or by both mechanisms (24–27). However, it is also possible that differences in β -catenin levels are not directly regulated by Nf1, but instead are a consequence of differences in cell differentiation, as mesenchymal cells in a less differentiated state may be characterized by higher β -catenin levels (28–31). Thus, a shift away from osteoblasts to undifferentiated mesenchymal cells could be responsible for the observed increase in β -catenin at the fracture site.

During the initial phases of fracture repair and during development, β -catenin needs to be precisely regulated for cells to become osteoblasts (12, 32). Our data suggest that NF1 tibial pseudarthrosis is at least in part caused by elevated levels of β -catenin preventing osteoblastic differentiation. Once cells are committed to the osteochondral lineage, deletion of β -catenin blocks osteoblast differentiation, shifting the process to chondrocyte formation. Thus, later in fracture repair, β -catenin could improve osteogenesis, but this can occur only if the appropriate osteochondral precursors are present. Our data support the notion that there is a deficient number of these precursors in NF1, because of the high levels of β -catenin. Thus, the phenotype we observed in NF1 pseudarthrosis is consistent with activation of β -catenin, leaving more undifferentiated mesenchymal cells and fibrous tissue at the fracture site.

Studies of impaired bone repair in NF1 have often focused on isolated signaling cascades without taking other relevant signaling pathways into account. Activation and maintenance of osteoblastogenesis is governed by a sophisticated network of partially converged pathways. Inhibition of TGF- β signaling has been shown capable of rescuing the nonunion and bone defects in a mouse model of NF1 (33). The reciprocal and synergic effects of Wnt/ β -catenin and TGF- β signaling pathways in the differentiation of MSCs to osteoblasts and chondrocytes (34–36) could explain the defective NF1 pseudarthrosis phenotype. Van den Bosche *et al.* (37) also showed that Wnt/ β -catenin stimulation skewed TGF- β signaling, resulting in chondrocyte hypertrophy, suggesting an alternative explanation for the abundance of hypertrophic chondrocytes in the defective NF1 pseudarthrosis tissue and at the site of fracture in NF1 murine models. On the other hand, hyperactive Ras/MAPK signaling has been identified as a critical

factor underlying the pathogenesis of NF1 pseudarthrosis and impaired fracture repair in NF1 mouse models (7). Activation of Ras signaling has been associated with LDL receptor protein-6-mediated activation of Wnt/ β -catenin in colorectal cancer (38) and activation of another member of the MAPK family, Rac1; control Wnt activation; and β -catenin nuclear localization during osteoblast differentiation (39). Our results from the Ad-Dkk1 treatment experiments also support the concept of receptor-mediated activation of Wnt/ β -catenin in NF1 fracture healing. Moreover, Rac1 has also been identified as a critical contributor in hyperactive osteoclasts in *Nf1* haploinsufficient mice (40); therefore, it could contribute to the NF1-defective osteoblastogenesis and osteoclast hyperactivity.

Osteoclastogenesis can be activated by RAS signaling, such as occurs in *Nf1* deficiency (5, 11, 41–50). We observed a gain in the number of osteoclasts at the *Nf1*-null murine fracture site, in agreement with previous studies (51–57). *In vitro* studies have shown a biphasic effect of β -catenin on osteoclast proliferation and differentiation (58). In our experiments, reducing β -catenin levels at the *Nf1*-null fracture site reduced the number of osteoclasts. This decrease could be caused by direct or indirect effects of Wnt/ β -catenin signaling on osteoclastogenesis, as suggested in other studies (59, 60). The potential role of β -catenin on osteoclast differentiation, particularly in NF1, warrants further research.

We demonstrated the potential utility of Dkk1 in restoring a more normal fracture-healing phenotype in NF1. The transient and targeted infection of Dkk1 at the site of *Nf1*-null fractures led to a greater increase in the number of osteoblasts, than knocking down β -catenin. Biomechanical testing revealed a restoration of mechanical stability to the fractured bone with an improvement in torsional stiffness and torque. Based on our data, we propose using therapy that alters β -catenin levels in clinical trials to improve bone repair in NF1 or as an adjunct for the treatment of congenital pseudarthrosis. FJ

The authors thank the families involved in this study and the NF Society of Ontario (NFSO) for their kind contribution and participation. This study was funded by Grant W81XWH-13-1-0113 from the U.S. Army Medical Research Acquisition Activity. Author contributions: S. Ghadakzadeh and B. A. Alman designed the study; S. Ghadakzadeh and H. Whetstone performed the research; and S. Ghadakzadeh, P. Kannu, A. Howard, and B. A. Alman analyzed the data and wrote the paper. The authors declare no conflicts of interest.

REFERENCES

1. Cho, T. J., Seo, J. B., Lee, H. R., Yoo, W. J., Chung, C. Y., and Choi, I. H. (2008) Biologic characteristics of fibrous hamartoma from congenital pseudarthrosis of the tibia associated with neurofibromatosis type 1. *J. Bone Joint Surg. Am.* **90**, 2735–2744
2. Ippolito, E., Corsi, A., Grill, F., Wientroub, S., and Bianco, P. (2000) Pathology of bone lesions associated with congenital pseudarthrosis of the leg. *J. Pediatr. Orthop.* **B9**, 3–10
3. El Khassawna, T., Toben, D., Kolanczyk, M., Schmidt-Bleek, K., Koennecke, I., Schell, H., Mundlos, S., and Duda, G. N. (2012) Deterioration of fracture healing in the mouse model of NF1 long bone dysplasia. *Bone* **51**, 651–660
4. El-Hoss, J., Sullivan, K., Cheng, T., Yu, N. Y., Bobyn, J. D., Peacock, L., Mikulec, K., Baldock, P., Alexander, I. E., Schindeler, A., and Little,

- D. G. (2012) A murine model of neurofibromatosis type I tibial pseudarthrosis featuring proliferative fibrous tissue and osteoclast-like cells. *J. Bone Miner. Res.* **27**, 68–78
5. Lee, S. M., Choi, I. H., Lee, D. Y., Lee, H. R., Park, M. S., Yoo, W. J., Chung, C. Y., and Cho, T. J. (2012) Is double inactivation of the Nf1 gene responsible for the development of congenital pseudarthrosis of the tibia associated with Nf1? *J. Orthop. Res.* **30**, 1535–1540
 6. Paria, N., Cho, T. J., Choi, I. H., Kamiya, N., Kayembe, K., Mao, R., Margraf, R. L., Obermossner, G., Oxendine, I., Sant, D. W., Song, M. H., Stevenson, D. A., Viskochil, D. H., Wise, C. A., Kim, H. K., and Rios, J. J. (2014) Neurofibromin deficiency-associated transcriptional dysregulation suggests a novel therapy for tibial pseudarthrosis in Nf1. *J. Bone Miner. Res.* **29**, 2636–2642
 7. Sharma, R., Wu, X., Rhodes, S. D., Chen, S., He, Y., Yuan, J., Li, J., Yang, X., Li, X., Jiang, L., Kim, E. T., Stevenson, D. A., Viskochil, D., Xu, M., and Yang, F. C. (2013) Hyperactive Ras/MAPK signaling is critical for tibial nonunion fracture in neurofibromin-deficient mice. *Hum. Mol. Genet.* **22**, 4818–4828
 8. El-Hoss, J., Cheng, T., Carpenter, E. C., Sullivan, K., Deo, N., Mikulec, K., Little, D. G., and Schindeler, A. (2014) A combination of rhBMP-2 (recombinant human bone morphogenetic protein-2) and MEK (MAP kinase/ERK Kinase) inhibitor PD0325901 increases bone formation in a murine model of neurofibromatosis type I pseudarthrosis. *J. Bone Joint Surg. Am.* **96**, e117
 9. American College of Physicians; American Physiological Society. (2006) Pathophysiology of neurofibromatosis type I. *Ann. Intern. Med.* **144**, 842–849
 10. Wu, X., Estwick, S. A., Chen, S., Yu, M., Ming, W., Nebesio, T. D., Li, Y., Yuan, J., Kapur, R., Ingram, D., Yoder, M. C., and Yang, F. C. (2006) Neurofibromin plays a critical role in modulating osteoblast differentiation of mesenchymal stem/progenitor cells. *Hum. Mol. Genet.* **15**, 2837–2845
 11. Yang, F. C., Chen, S., Robling, A. G., Yu, X., Nebesio, T. D., Yan, J., Morgan, T., Li, X., Yuan, J., Hock, J., Ingram, D. A., and Clapp, D. W. (2006) Hyperactivation of p21ras and PI3K cooperate to alter murine and human neurofibromatosis type I-haploinsufficient osteoclast functions. *J. Clin. Invest.* **116**, 2880–2891
 12. Chen, Y., and Alman, B. A. (2009) Wnt pathway, an essential role in bone regeneration. *J. Cell. Biochem.* **106**, 353–362
 13. Chen, Y., Whetstone, H. C., Lin, A. C., Nadesan, P., Wei, Q., Poon, R., and Alman, B. A. (2007) Beta-catenin signaling plays a disparate role in different phases of fracture repair: implications for therapy to improve bone healing. *PLoS Med.* **4**, e249
 14. Zhu, Y., Romero, M. I., Ghosh, P., Ye, Z., Charnay, P., Rushing, E. J., Marth, J. D., and Parada, L. F. (2001) Ablation of Nf1 function in neurons induces abnormal development of cerebral cortex and reactive gliosis in the brain. *Genes Dev.* **15**, 859–876
 15. Harada, N., Tamai, Y., Ishikawa, T., Sauer, B., Takaku, K., Oshima, M., and Taketo, M. M. (1999) Intestinal polyposis in mice with a dominant stable mutation of the beta-catenin gene. *EMBO J.* **18**, 5931–5942
 16. Brault, V., Moore, R., Kutsch, S., Ishibashi, M., Rowitch, D. H., McMahon, A. P., Sommer, L., Boussadia, O., and Kemler, R. (2001) Inactivation of the beta-catenin gene by Wnt1-Cre-mediated deletion results in dramatic brain malformation and failure of craniofacial development. *Development* **128**, 1253–1264
 17. Kuhnert, F., Davis, C. R., Wang, H. T., Chu, P., Lee, M., Yuan, J., Nusse, R., and Kuo, C. J. (2004) Essential requirement for Wnt signaling in proliferation of adult small intestine and colon revealed by adenoviral expression of Dickkopf-1. *Proc. Natl. Acad. Sci. USA* **101**, 266–271
 18. Parfitt, A. M. (1988) Bone histomorphometry: standardization of nomenclature, symbols and units. Summary of proposed system. *Bone Miner.* **4**, 1–5
 19. Schneider, C. A., Rasband, W. S., and Eliceiri, K. W. (2012) NIH Image to ImageJ: 25 years of image analysis. *Nat. Methods* **9**, 671–675
 20. Rosa, A. L., and Beloti, M. M. (2005) Development of the osteoblast phenotype of serial cell subcultures from human bone marrow. *Braz. Dent. J.* **16**, 225–230
 21. Lee, D. Y., Cho, T. J., Lee, H. R., Lee, K., Moon, H. J., Park, M. S., Yoo, W. J., Chung, C. Y., and Choi, I. H. (2011) Disturbed osteoblastic differentiation of fibrous hamartoma cell from congenital pseudarthrosis of the tibia associated with neurofibromatosis type I. *Clin. Orthop. Surg.* **3**, 230–237
 22. Leskelä, H. V., Kuorilehto, T., Risteli, J., Koivunen, J., Nissinen, M., Peltonen, S., Kinnunen, P., Messiaen, L., Lehenkari, P., and Peltonen, J. (2009) Congenital pseudarthrosis of neurofibromatosis type I: impaired osteoblast differentiation and function and altered Nf1 gene expression. *Bone* **44**, 243–250
 23. Cheon, S. S., Wei, Q., Gurung, A., Youn, A., Bright, T., Poon, R., Whetstone, H., Guha, A., and Alman, B. A. (2006) Beta-catenin regulates wound size and mediates the effect of TGF-beta in cutaneous healing. *FASEB J.* **20**, 692–701
 24. Sharma, M., Chuang, W. W., and Sun, Z. (2002) Phosphatidylinositol 3-kinase/Akt stimulates androgen pathway through GSK3beta inhibition and nuclear beta-catenin accumulation. *J. Biol. Chem.* **277**, 30935–30941
 25. Fang, D., Hawke, D., Zheng, Y., Xia, Y., Meisenhelder, J., Nika, H., Mills, G. B., Kobayashi, R., Hunter, T., and Lu, Z. (2007) Phosphorylation of beta-catenin by AKT promotes beta-catenin transcriptional activity. *J. Biol. Chem.* **282**, 11221–11229
 26. Cross, D. A., Alessi, D. R., Cohen, P., and Andjelkovich, M., and Hemmings, B. A. (1995) Inhibition of glycogen synthase kinase-3 by insulin mediated by protein kinase B. *Nature* **378**, 785–789
 27. Srivastava, A. K., and Pandey, S. K. (1998) Potential mechanism(s) involved in the regulation of glycogen synthesis by insulin. *Mol. Cell. Biochem.* **182**, 135–141
 28. Sato, N., Meijer, L., Skaltsounis, L., Greengard, P., and Brivanlou, A. H. (2004) Maintenance of pluripotency in human and mouse embryonic stem cells through activation of Wnt signaling by a pharmacological GSK-3-specific inhibitor. *Nat. Med.* **10**, 55–63
 29. Anton, R., Kestler, H. A., and Kühl, M. (2007) Beta-catenin signaling contributes to stemness and regulates early differentiation in murine embryonic stem cells. *FEBS Lett.* **581**, 5247–5254
 30. Sokol, S. Y. (2011) Maintaining embryonic stem cell pluripotency with Wnt signaling. *Development* **138**, 4341–4350
 31. Etheridge, S. L., Spencer, G. J., Heath, D. J., and Genever, P. G. (2004) Expression profiling and functional analysis of Wnt signaling mechanisms in mesenchymal stem cells. *Stem Cells* **22**, 849–860
 32. Hadjiargyrou, M., Lombardo, F., Zhao, S., Ahrens, W., Joo, J., Ahn, H., Jurman, M., White, D. W., and Rubin, C. T. (2002) Transcriptional profiling of bone regeneration: insight into the molecular complexity of wound repair. *J. Biol. Chem.* **277**, 30177–30182
 33. Rhodes, S. D., Wu, X., He, Y., Chen, S., Yang, H., Staser, K. W., Wang, J., Zhang, P., Jiang, C., Yokota, H., Dong, R., Peng, X., Yang, X., Murthy, S., Azhar, M., Mohammad, K. S., Xu, M., Guise, T. A., and Yang, F. C. (2013) Hyperactive transforming growth factor-beta1 signaling potentiates skeletal defects in a neurofibromatosis type I mouse model. *J. Bone Miner. Res.* **28**, 2476–2489
 34. Wu, M., Chen, G., and Li, Y.-P. (2016) TGF-β and BMP signaling in osteoblast, skeletal development, and bone formation, homeostasis and disease. *Bone Res.* **4**, 16009
 35. Chen, G., Deng, C., and Li, Y. P. (2012) TGF-β and BMP signaling in osteoblast differentiation and bone formation. *Int. J. Biol. Sci.* **8**, 272–288
 36. McCarthy, T. L., and Centrella, M. (2010) Novel links among Wnt and TGF-beta signaling and Runx2. *Mol. Endocrinol.* **24**, 587–597
 37. van den Bosch, M. H., Blom, A. B., van Lent, P. L., van Beuningen, H. M., Blaney Davidson, E. N., van der Kraan, P. M., and van den Berg, W. B. (2014) Canonical Wnt signaling skews TGF-β signaling in chondrocytes towards signaling via ALK1 and Smad 1/5/8. *Cell. Signal.* **26**, 951–958
 38. Lemieux, E., Cagnol, S., Beaudry, K., Carrier, J., and Rivard, N. (2015) Oncogenic KRAS signalling promotes the Wnt/β-catenin pathway through LRP6 in colorectal cancer. *Oncogene* **34**, 4914–4927
 39. Wu, X., Tu, X., Joeng, K. S., Hilton, M. J., Williams, D. A., and Long, F. (2008) Rac1 activation controls nuclear localization of beta-catenin during canonical Wnt signaling. *Cell* **133**, 340–353
 40. Yan, J., Chen, S., Zhang, Y., Li, X., Li, Y., Wu, X., Yuan, J., Robling, A. G., Kapur, R., Chan, R. J., and Yang, F. C. (2008) Rac1 mediates the osteoclast gains-in-function induced by haploinsufficiency of Nf1. *Hum. Mol. Genet.* **17**, 936–948
 41. Li, H., Liu, Y., Zhang, Q., Jing, Y., Chen, S., Song, Z., Yan, J., Li, Y., Wu, X., Zhang, X., Zhang, Y., Case, J., Yu, M., Ingram, D. A., and Yang, F. C. (2009) Ras dependent paracrine secretion of osteopontin by Nf1+/- osteoblasts promote osteoclast activation in a neurofibromatosis type I murine model. *Pediatr. Res.* **65**, 613–618
 42. Le, L. Q., and Parada, L. F. (2007) Tumor microenvironment and neurofibromatosis type I: connecting the GAPs. *Oncogene* **26**, 4609–4616
 43. Lammert, M., Friedman, J. M., Kluge, L., and Mautner, V. F. (2005) Prevalence of neurofibromatosis I in German children at elementary school enrollment. *Arch. Dermatol.* **141**, 71–74
 44. Kuorilehto, T., Pöyhönen, M., Bloigu, R., Heikkinen, J., Väänänen, K., and Peltonen, J. (2005) Decreased bone mineral density and content

- in neurofibromatosis type 1: lowest local values are located in the load-carrying parts of the body. *Osteoporos. Int.* **16**, 928–936
45. Kuorilehto, T., Nissinen, M., Koivunen, J., Benson, M. D., and Peltonen, J. (2004) NF1 tumor suppressor protein and mRNA in skeletal tissues of developing and adult normal mouse and NF1-deficient embryos. *J. Bone Miner. Res.* **19**, 983–989
 46. Johnston II, C. E. (2002) Congenital pseudarthrosis of the tibia: results of technical variations in the charnley-williams procedure. *J. Bone Joint Surg. Am.* **84-A**, 1799–1810
 47. Heervä, E., Peltonen, S., Svedström, E., Aro, H. T., Väänänen, K., and Peltonen, J. (2012) Osteoclasts derived from patients with neurofibromatosis 1 (NF1) display insensitivity to bisphosphonates in vitro. *Bone* **50**, 798–803
 48. Stevenson, D. A., Schwarz, E. L., Carey, J. C., Viskochil, D. H., Hanson, H., Bauer, S., Weng, H. Y., Greene, T., Reinker, K., Swensen, J., Chan, R. J., Yang, F. C., Senbanjo, L., Yang, Z., Mao, R., and Pasquali, M. (2011) Bone resorption in syndromes of the Ras/MAPK pathway. *Clin. Genet.* **80**, 566–573
 49. Heervä, E., Alanne, M. H., Peltonen, S., Kuorilehto, T., Hentunen, T., Väänänen, K., and Peltonen, J. (2010) Osteoclasts in neurofibromatosis type 1 display enhanced resorption capacity, aberrant morphology, and resistance to serum deprivation. *Bone* **47**, 583–590
 50. Wang, W., Nyman, J. S., Moss, H. E., Gutierrez, G., Mundy, G. R., Yang, X., and Eleferiou, F. (2010) Local low-dose lovastatin delivery improves the bone-healing defect caused by Nf1 loss of function in osteoblasts. *J. Bone Miner. Res.* **25**, 1658–1667
 51. Schindeler, A., and Little, D. G. (2008) Recent insights into bone development, homeostasis, and repair in type 1 neurofibromatosis (NF1). *Bone* **42**, 616–622
 52. Schindeler, A., Birke, O., Yu, N. Y., Morse, A., Ruys, A., Baldock, P. A., and Little, D. G. (2011) Distal tibial fracture repair in a neurofibromatosis type 1-deficient mouse treated with recombinant bone morphogenetic protein and a bisphosphonate. *J. Bone Joint Surg. Br.* **93**, 1134–1139
 53. Liu, R., Birke, O., Morse, A., Peacock, L., Mikulec, K., Little, D. G., and Schindeler, A. (2011) Myogenic progenitors contribute to open but not closed fracture repair. *BMC Musculoskelet. Disord.* **12**, 288
 54. El-Hoss, J., Sullivan, K., Cheng, T., Yu, N. Y., Bobyn, J. D., Peacock, L., Mikulec, K., Baldock, P., Alexander, I. E., Schindeler, A., and Little, D. G. (2012) A murine model of neurofibromatosis type 1 tibial pseudarthrosis featuring proliferative fibrous tissue and osteoclast-like cells. *J. Bone Miner. Res.* **27**, 68–70
 55. Eleferiou, F., Kolanczyk, M., Schindeler, A., Viskochil, D. H., Hock, J. M., Schorry, E. K., Crawford, A. H., Friedman, J. M., Little, D., Peltonen, J., Carey, J. C., Feldman, D., Yu, X., Armstrong, L., Birch, P., Kendler, D. L., Mundlos, S., Yang, F. C., Agiostratidou, G., Hunter-Schaedle, K., and Stevenson, D. A. (2009) Skeletal abnormalities in neurofibromatosis type 1: approaches to therapeutic options. *Am. J. Med. Genet. A.* **149**, 2327–2338
 56. Dulai, S., Briody, J., Schindeler, A., North, K. N., Cowell, C. T., and Little, D. G. (2007) Decreased bone mineral density in neurofibromatosis type 1: results from a pediatric cohort. *J. Pediatr. Orthop.* **27**, 472–475
 57. Birke, O., Schindeler, A., Ramachandran, M., Cowell, C. T., Munns, C. F., Bellemore, M., and Little, D. G. (2010) Preliminary experience with the combined use of recombinant bone morphogenetic protein and bisphosphonates in the treatment of congenital pseudarthrosis of the tibia. *J. Child. Orthop.* **4**, 507–517
 58. Wei, W., Zeve, D., Suh, J. M., Wang, X., Du, Y., Zerwekh, J. E., Dechow, P. C., Graff, J. M., and Wan, Y. (2011) Biphasic and dosage-dependent regulation of osteoclastogenesis by β -catenin. *Mol. Cell. Biol.* **31**, 4706–4719
 59. Jang, H. D., Shin, J. H., Park, D. R., Hong, J. H., Yoon, K., Ko, R., Ko, C. Y., Kim, H. S., Jeong, D., Kim, N., and Lee, S. Y. (2011) Inactivation of glycogen synthase kinase-3 β is required for osteoclast differentiation. *J. Biol. Chem.* **286**, 39043–39050
 60. Weivoda, M. M., Ruan, M., Hachfeld, C. M., Pederson, L., Howe, A., Davey, R. A., Zajac, J. D., Kobayashi, Y., Williams, B. O., Westendorf, J. J., Khosla, S., and Oursler, M. J. (2016) Wnt signaling inhibits osteoclast differentiation by activating canonical and noncanonical cAMP/PKA pathways. *J. Bone Miner. Res.* **31**, 65–75

Received for publication December 30, 2015.
Accepted for publication May 31, 2017.

β -Catenin modulation in neurofibromatosis type 1 bone repair: therapeutic implications

Saber Ghadakzadeh, Peter Kannu, Heather Whetstone, et al.

FASEB J 2016 30: 3227-3237 originally published online June 15, 2016

Access the most recent version at doi:[10.1096/fj.201500190RR](https://doi.org/10.1096/fj.201500190RR)

Supplemental Material <http://www.fasebj.org/content/suppl/2016/06/15/fj.201500190RR.DC1.html>

References This article cites 59 articles, 17 of which can be accessed free at:
<http://www.fasebj.org/content/30/9/3227.full.html#ref-list-1>

Subscriptions Information about subscribing to *The FASEB Journal* is online at
<http://www.faseb.org/The-FASEB-Journal/Librarian-s-Resources.aspx>

Permissions Submit copyright permission requests at:
<http://www.fasebj.org/site/misc/copyright.xhtml>

Email Alerts Receive free email alerts when new an article cites this article - sign up at
<http://www.fasebj.org/cgi/alerts>

α -GalCer now available
C8, C16 & C24:1 Galactosyl(α) Ceramide



Avanti[®]
POLAR LIPIDS, INC.